EvoPrompting: Language Models for Code-Level Neural Architecture Search

Angelica Chen [1 2]   David M. Dohan [* 3]   David R. So [* 3]

Abstract

Given the recent impressive accomplishments of language models (LMs) for code generation, we explore the use of LMs as general adaptive mutation and crossover operators for an evolutionary neural architecture search (NAS) algorithm. While NAS still proves too difficult a task for LMs to succeed at solely through prompting, we find that the combination of evolutionary prompt engineering with soft prompt tuning, a method we term EVOPROMPTING, consistently finds diverse and high performing models. We first demonstrate that EVOPROMPTING is effective on the computationally efficient MNIST-1D dataset, where EVO-PROMPTING produces convolutional architecture variants that outperform both those designed by human experts and naive few-shot prompting in terms of accuracy and model size. We then apply our method to searching for graph neural networks on the CLRS Algorithmic Reasoning Benchmark, where EVOPROMPTING is able to design *novel* architectures that outperform current state-of-the-art models on 21 out of 30 algorithmic reasoning tasks while maintaining similar model size. EVOPROMPTING is successful at designing accurate and efficient neural network architectures across a variety of machine learning tasks, while also being general enough for easy adaptation to other tasks beyond neural network design.

1. Introduction

Scaling of Transformers (Vaswani et al., 2017) has produced language models (LM) with impressive performance. Beyond achieving state-of-the-art results on conventional natural language processing tasks, these LMs demonstrate breakthrough technical capabilities, such as learning how

*Equal contribution [1]Center for Data Science, New York University, New York, USA [2]Work done while a Student Researcher at Google Brain. [3]Google Brain. Correspondence to: Angelica Chen <angelica.chen@nyu.edu>, David So <davidso@google.com>.
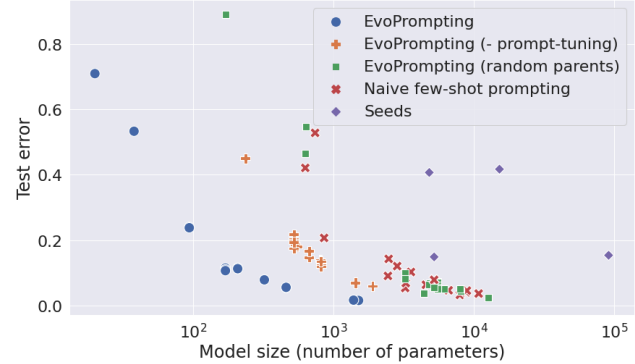
Figure 1. EVOPROMPTING, which combines evolutionary search with soft-prompt tuning, discovers smaller and better performing architectures on MNIST1D than alternative search methods.

to code (Chen et al., 2021), doing math (Noorbakhsh et al., 2021), and solving reasoning problems (Wei et al., 2022).

Yet, despite these strides, several works have noted LMs' current limitations in solving complex problems and creating novel solutions (Qian et al., 2022; Dakhel et al., 2022). In this work, we improve upon a base LM's ability to propose novel and diverse solutions to complex reasoning problems by iteratively evolving in-context prompts and prompt-tuning the LM. We call this technique EVOPROMPTING and demonstrate its success on the narrow but difficult task of deep learning architecture design. Our key finding is that, while LMs largely fail at designing novel and effective neural architectures via naive few-shot prompting, EVO-PROMPTING enables LMs to create novel and effective deep neural architectures, particularly when combined with prompt-tuning methods.

EVOPROMPTING is based on the recently popularized practice of in-context prompting. Prompting is the technique of conditioning a LM's decoded output on a custom prefix known as a *prompt*, which can include natural language task instructions or a few input-output examples. The prompt is used only at inference time and requires no gradient updates (Brown et al., 2020). In past work, prompting has been demonstrated to elicit impressive performance on a wide variety of tasks without requiring task-specific fine-tuning (Sanh et al., 2021; Wei et al., 2022; Kojima et al., 2022). Here, we leverage LM prompting for the task of designing improved deep learning architectures.
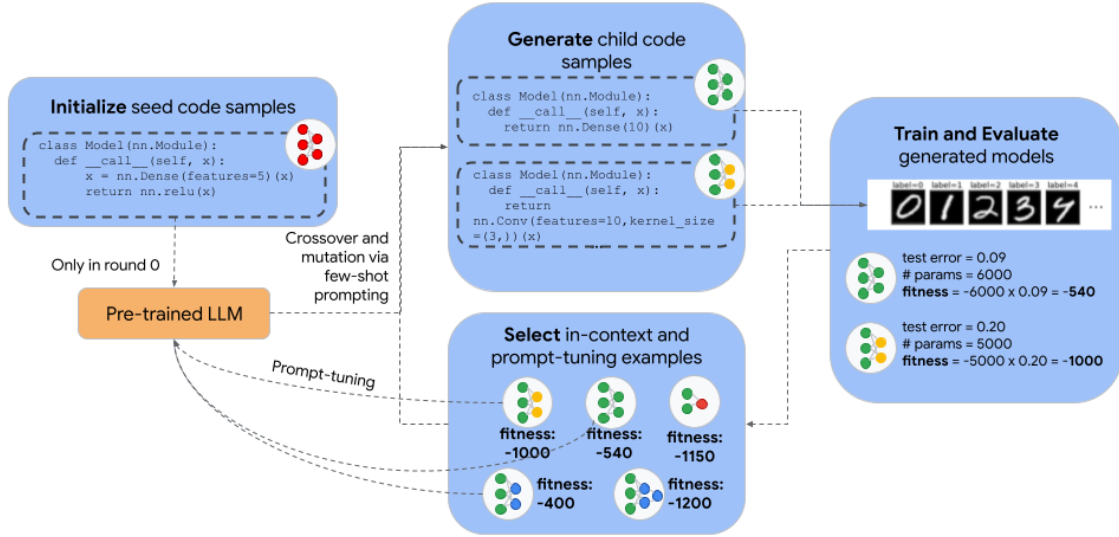
Figure 2. An overview of EVOPROMPTING. After *initializing* the search with a handful of manually designed program seeds, the meta-learning loop begins. First, our code-pretrained LM uses the seeds as in-context prompt examples to *generate* candidate architectures. Those candidate architectures are then *trained* on the task training data and *evaluated* on the task validation set. Next, the most fit members of the population are *selected* as in-context examples for the next meta-learning loop and all evaluated individuals are used as training data for prompt-tuning the LM. From there, the meta-learning loop begins again.

To engineer adequately powerful prompts, we draw inspiration from existing ideas in the field of neural architecture search. There, evolution has long been used to search over discrete spaces to efficiently discover improved deep learning architectures (Yao, 1999; Real et al., 2017). However, evolutionary approaches typically require careful manual design of a discrete search space (*e.g.* a small set of known convolutional neural network components, as in Real et al. (2017) or TensorFlow primitives, as in So et al. (2021)). As a result, the performance of the evolutionary algorithm is then sensitive to and possibly limited by the design of the search space. In EVOPROMPTING the LM's vocabulary replaces the search space, which both increases the flexibility of the search and reduces reliance on manual design. The LM is also an *adaptive* mutation/crossover operator, in the sense that it can be improved round over round via prompt-tuning. Furthermore, EVOPROMPTING also improves on naive few-shot prompting by using an evolutionary search approach to iteratively improve the in-context examples for few-shot prompting.

To demonstrate the effectiveness of this method, we first do extensive testing and analyses on the relatively low-compute problem of MNIST-1D (Greydanus, 2020). The key finding of these experiments is that EVOPROMPTING is capable of producing conventional convolutional architectures supe-

rior to published manually designed models. In Section 4.2 we then apply our method to the more challenging task of designing graph neural networks using problems from the CLRS Algorithmic Reasoning Benchmark (Veličković et al., 2022). There, EVOPROMPTING generates novel architectures and modules that outperform state-of-the-art models on 21 out of 30 algorithmic tasks (Appx. A.5).

The contributions of this work are summarized as follows:

1. We propose EVOPROMPTING, a method that utilizes evolutionary search to create and curate data to improve LM in-context prompting examples. Although this work focuses on the specific task of neural architecture design to develop this method, EVOPROMPTING is generally applicable to LM tasks that rely on in-context learning or prompt-tuning.

2. A study applying LMs to code-level neural architecture design. Our experiments demonstrate that applying few-shot prompting alone to neural architecture design is unsuccessful, but few-shot prompting with EVOPROMPTING enables LMs to create architectures that outperform those designed by human experts.

3. Novel graph neural network architectures that were discovered using EVOPROMPTING. These architec-

tures outperform the current state-of-the-art architecture, Triplet-GMPNN (Ibarz et al., 2022), on 21 out of 30 CLRS Algorithmic Reasoning Benchmark tasks (Appx. A.5).

2. Related Work

LMs for code generation Scaling Transformers (Vaswani et al., 2017) is currently the most popular route for reliably creating state-of-the-art natural language systems (Brown et al., 2020; Du et al., 2021; BigScience Workshop et al., 2022; Zhang et al., 2022; Thoppilan et al., 2022; Chowdhery et al., 2022). Many works have observed that these LM systems are capable of performing technical tasks such as writing code (Chen et al., 2021), doing math (Noorbakhsh et al., 2021), and solving reasoning problems (Wei et al., 2022). Our work is most closely related to efforts that have applied LMs to coding tasks (Chen et al., 2021; Odena et al., 2021; Xu et al., 2022; Wang et al., 2021; Ahmad et al., 2021; Feng et al., 2020), since our technique proposes architectures in code.

Prompting Brown et al. (2020) critically demonstrated that LMs can be prompted with in-context examples to steer LM decoding towards solving specific problems, potentially unseen in the training data. Numerous works have utilized this prompting to further unlock latent LM abilities (Sanh et al., 2021; Wei et al., 2022; Kojima et al., 2022). In this work, we employ prompting to guide our LMs to perform neural architecture design. Because this prompting is critical to LM performance, numerous works have analyzed prompting and proposed different prompt engineering strategies (Min et al., 2022; Liu et al., 2021). Examples include works using retrieval systems to augment prompts (Rubin et al., 2021), determining optimal few-shot permutations (Lu et al., 2021; Zhao et al., 2021), employing LMs to create natural language prompts (Zhou et al., 2022), and including prompt templating in weight training to improve in-context learning (Wei et al., 2021; Ouyang et al., 2022; Sanh et al., 2021). From the perspective of Dohan et al. (2022), prompts are parameters and may be tuned using a variety of probabilistic inference techniques. Brooks et al. (2022) proposes using these prompts to implement both the rollout policy and world model of a policy iteration algorithm, where the in-context examples are selected to be the most relevant towards the current inference. Our EVOPROMPTING method extends these efforts by proposing evolutionary search as a means to better design prompts for in-context learning.

Evolutionary Algorithms The way in which we use evolution to iteratively improve our in-context example architectures is closely related to evolutionary neural architecture search (NAS) (Real et al., 2017; 2018; Elsken et al., 2018; So et al., 2019; Liu et al., 2020). In evolutionary NAS,

architecture design is posed as a search problem – architectures are represented as discrete DNAs and evolved based on fitness metrics that assess architecture performance, resulting in a final population of high quality architectures. Our method follows a similar approach, but with our LM replacing two key components. Firstly, the search space is defined over arbitrary strings, represented using the LM's SentencePiece tokens (Kudo & Richardson, 2018). This stands in stark contrast to conventional NAS, which relies on hand-crafted search spaces, that can strongly bias and constrain the searches (Li & Talwalkar, 2019; Sciuto et al., 2019; Bender et al., 2020). Even in cases where much more open ended search spaces are used, these spaces still require human expertise to be designed and implemented (Real et al., 2020; So et al., 2021). In this work, any syntactically valid piece of code is covered in our search space; the only limitations are those imposed by the coding language and libraries (ex., Python and JAX). Secondly, the LM replaces the mutation and crossover functions that are commonly hand-designed (Koza, 1993). Not only does this reduce human bias, but it also allows the mutation and crossover functions to improve over the course of the search via prompt-tuning, as we demonstrate in Section 4.

A work close to ours is Lehman et al. (2022), in which an LM is first fine-tuned to produce Python code diffs given one of three fixed messages that describe what should be changed, and then used as the mutation operator in an evolutionary algorithm coupled with the MAP-Elites (Multi-dimensional Archive of Phenotypic-Elites) algorithm designed as a quality-diversity (QD) algorithm. Their work is validated on the Sodarace domain, a virtual game where an agent must navigate a robot through various race tracks. Our work differs in that we use an LM as a crossover operator, without specifying the class of changes to make, which may offer greater flexibility. Furthermore, we evaluate our approach on the real-world task of NAS, rely on mixed temperature sampling of the LM for diversity instead of using a QD algorithm, and also use prompt-tuning in our algorithm. We choose not to use a QD algorithm such as MAP-Elites since this approach requires the design and discretization of a descriptor space, which is complex and difficult to hand-design for the space of all possible neural networks.

A concurrent work, Meyerson et al. (2023), also uses an LM as a crossover operator to produce variations of text-based genotypes in the domains of symbolic regression, text sentiment, images, and Sodaracer programs. Like Lehman et al. (2022), they use MAP-Elites to trade off quality with diversity and demonstrate that their overall algorithm reliably produces a diverse range of outputs. Their study varies from ours in a number of ways - we additionally optimize for state-of-the-art task performance (rather than only diversity of outputs), we condition on target performance in our prompts, we do not use MAP-Elites, we use prompt-tuning

to iteratively improve the LM's crossover abilities, and we apply our algorithm to the real-world task of NAS instead.

Sequence models improving machine learning This work is not the first time that deep sequence models have been used to improve machine learning workflows. For example, Chen et al. (2022) applies Transformers to hyperparameter optimization and Zoph & Le (2016) uses recurrent neural networks to perform architecture search via reinforcement learning. Our work differs from these approaches in that our model's action space is not specifically crafted for our target task. Instead, we use a pre-trained LM with a conventional SentencePiece output vocabulary to generate Python code (Kudo & Richardson, 2018).

3. EVOPROMPTING Method

3.1. Architecture search problem formulation

Let our target task be denoted by $\mathcal{T}$ and $\mathcal{D}$ be a dataset consisting of input-output pairs $(x, y) \in \mathcal{D}$ for task $\mathcal{T}$. Define the probability distribution $\pi_\theta : \mathcal{V} \to \{0, 1\}$ over vocabulary $\mathcal{V}$ as a language/code model parameterized by θ, from which we can sample code segments $c \in \mathcal{V}^*$ (for $\mathcal{V}^*$ the Kleene closure of $\mathcal{V}$, *i.e.* the set of all finite concatenations of symbols in $\mathcal{V}$).

We also have an evaluation function $\text{EVAL}_\mathcal{T}(c, \mathcal{D}) : \mathcal{V}^* \times \mathcal{D} \to \mathbb{R}$ that trains the model architecture given by code c on $\mathcal{D}$ and outputs some real-valued fitness $s \in \mathbb{R}$, which can be a function of model accuracy and other model characteristics.

Our ultimate goal is to identify some set of code samples $c \sim \mathcal{V}^*$ that define neural network architectures that, when trained on $\mathcal{D}$, maximize the reward $\text{EVAL}_\mathcal{T}(c, \mathcal{D})$.

3.2. LMs for evolutionary crossover and mutation

The goal of our algorithm is to generate a set C consisting of k neural network architectures that maximize the reward $\text{EVAL}_\mathcal{T}(c, \mathcal{D})$ for arbitrary pairs of $(\mathcal{D}, \mathcal{T})$:

$$\arg \max_{\substack{C = \{c \,|\, c \sim \pi_\theta\} \\ |C| = k}} \mathbb{E}_{c \in C} \mathbb{E}_{(x,y) \in \mathcal{D}} \left[\text{EVAL}_\mathcal{T}(c, \mathcal{D}) \right] \quad (1)$$

Since this optimization problem is generally intractable, we turn to a black-box evolutionary approach for iteratively generating, scoring, and selecting the best neural network architectures. Indeed, evolution has been demonstrated to perform particularly well in this domain because of how sparse high quality solutions tend to be (Real et al., 2017; 2018). Although evolution has been used for architecture search many times before (Real et al., 2017; 2018; Elsken et al., 2018; So et al., 2019), we improve upon this approach by using an LM for crossover and mutation operations.

Using an LM in this manner has multiple appealing properties. While past evolutionary approaches for neural architecture search have required careful design and specification of a discrete search space (*e.g.* the space of high level modules (Real et al., 2018; So et al., 2019), TensorFlow statements (So et al., 2021), or basic mathematical operations (Real et al., 2020)), our algorithm's search space includes any neural network architecture that can be represented in Python. This allows for greater flexibility and diversity of the output architectures, and reduces the amount of manual design and human bias involved in the algorithm. Furthermore, modern pre-trained LMs are typically trained on massive datasets containing a significant number of source code files. This pre-training process encodes useful knowledge about code structure and functionality that is not otherwise available in evolutionary algorithms. Lastly, LMs can also be used as *self-adaptive crossover operators*, in which the crossover operator is incrementally trained round after round to generate higher reward crossovers.

1: **Input:** LM π_{θ_0}, dataset $\mathcal{D}$, task $\mathcal{T}$, T number of rounds, m number of few-shot prompts per round, n number of samples to generate per prompt, k number of in-context examples per prompt, p number of survivors to select per generation, α the upper threshold for the test error
2: $G \leftarrow []$
3: $P \leftarrow \text{INITIALIZEPOPULATION}(p)$
4: $t \leftarrow 0$
5: **while** $t < T$ **do**
6:     $C \leftarrow \text{CROSSMUT}(\pi_{\theta_t}, P, m, k, n)$
7:     $C_{\text{EVALED}} \leftarrow \text{FILTERANDEVAL}(C, \mathcal{T}, \mathcal{D}, \alpha)$
8:     $G \leftarrow G + C_{\text{EVALED}}$
9:     **if** $t < T - 1$ **then**
10:         $P \leftarrow \text{GETTOP}(G, p)$
11:         $\theta_{t+1} \leftarrow \text{TRAIN}(\theta_t, C_{\text{EVALED}} \setminus P)$
12:     **end if**
13:     $t \leftarrow t + 1$
14: **end while**
15: Return $\text{GETTOP}(G, p)$

Algorithm 1: Complete meta-learning evolutionary algorithm using p_θ as a crossover and mutation operator.

3.3. EVOPROMPTING meta-learning algorithm

Our complete algorithm is described in Algorithm 1. At the core of our algorithm is a scoring function, which describes the general "fitness" of a model on the task at hand. Since higher accuracy can often be achieved simply by increasing the number of parameters in a model, we use the negative product of the validation error and the model size as the fitness (see step 6 in Algorithm 3). More complicated objective functions have previously been used for dual objective neural architecture search (Bender et al., 2020), but we find

1: **Input:** LM π_θ, population of code samples and fitnesses $P = \{(c, s) \,|\, c \in \mathcal{V}^*, \text{EVAL}_\mathcal{T}(c, \mathcal{D}) = s\}$, m number of few-shot prompts to create, k number of in-context examples in each prompt, and n number of samples to sample per prompt.
2: $C \leftarrow []$
3: $i \leftarrow 0$
4: **while** $i < m$ **do**
5:     $E \leftarrow \{x_j\}_{j=1}^k$, where $x_j \overset{i.i.d.}{\sim} \text{Uniform}(P)$
6:     $p \leftarrow \text{MAKEFEWSHOTPROMPT}(E)$
7:     $C_i \leftarrow \{c_j\}_{j=1}^n$, where $c_j \overset{i.i.d.}{\sim} \pi_\theta(\cdot \,|\, p)$
8:     $C \leftarrow C + C_i$
9:     $i \leftarrow i + 1$
10: **end while**
11: **Output:** C

Algorithm 2: The crossover and mutation algorithm, $\text{CROSSMUT}(\pi_{\theta_t}, P, m, k, n)$, where $\text{Uniform}(P)$ denotes the uniform distribution over the set P. The set of potential parents P consists of the top examples from the previous round.

1: **Input:** set of code samples C, task $\mathcal{T}$, dataset $\mathcal{D}$, evaluation function $\text{EVAL}_\mathcal{T}(c, \mathcal{D})$, upper threshold for error α
2: $C_{\text{EVALED}} \leftarrow []$
3: **for** c in C **do**
4:     c.error $\leftarrow \text{EVAL}_\mathcal{T}(c, \mathcal{D})$
5:     **if** c.error $< \alpha$ **then**
6:        $s \leftarrow -$c.model_size $\times$ c.error
7:        $C_{\text{EVALED}} \leftarrow C_{\text{EVALED}} + [(c, s)]$
8:     **end if**
9: **end for**
10: **Output:** C_{EVALED}

Algorithm 3: The algorithm for filtering and scoring child models, $\text{FILTERANDEVAL}(C, \mathcal{T}, \mathcal{D}, \alpha)$.

this simple product works best in our case and requires minimal tuning. Generally the higher the fitness, the better (with some caveats, noted in our description of fitness-based selection below).

The end-to-end meta-learning algorithm has several stages, which we describe below:

Initialization   We start by setting our global historical population G to the empty list and initializing our current population P with a few seed architectures that are known to be well-designed (step 3 in Algorithm 1), which *warm-starts* the search (So et al., 2019). These seed models are evaluated using the same $\text{EVAL}_\mathcal{T}(c, \mathcal{D})$ function that is used to evaluate new candidate models (see below).

Crossing over and mutating the parent models   To mutate and apply crossover to the parents P selected in the last step, we use both the source code and the evaluation metrics of each model in P to create few-shot prompts.

In the last line of the prompt, we create a target set of metrics to condition π_θ's generations on that indicate the desired validation accuracy and model size of the proposed architecture. We set the target model size as 90% of the minimum model size of the parent models, rounded to the nearest 100 parameters, and the target validation accuracy as 102% of the maximum validation accuracy of the parent models, rounded to the nearest tenth of a percent. We create m such prompts per round, each with k in-context examples selected uniformly at random from P. An example of a prompt might look like the following:

```
1  """Metrics:
2  {'num_params': '4800', 'val_accuracy
       ': '0.865'}
3  """
4  class Model(nn.Module):
5    @nn.compact
6    def __call__(self, x):
7      x = nn.Dense(features=10)(x)
8      return x
9
10   """Metrics:
11  {'num_params': '4300', 'val_accuracy
       ': '0.880'}
12  """
13  class Model(nn.Module):
```

Listing 1. An example of a few-shot prompt. In practice we use 2-shot prompts but we omit the second in-context example here for brevity.

Finally, we use π_θ to generate n samples per prompt, yielding a total of $n \times m$ child samples per round of evolution. We denote this portion of the algorithm as $\text{CROSSMUT}(\pi_{\theta_t}, P, m, k, n)$ (Algorithm 2 and step 6 of Algorithm 1).

Filtering and scoring child samples   To score and filter child samples c generated by π_θ, we use the evaluation function $\text{EVAL}_\mathcal{T}(c, \mathcal{D})$, which trains the model encoded by c on the dataset $\mathcal{D}$ and returns the lowest validation error encountered during training. All child models are trained for the same number of steps, with the same optimizer hyperparameters. Since our fitness function can potentially be gamed by generating arbitrarily small models, we also add a validation error threshold α, which is the upper limit of the validation error that a model can incur without being removed from G, the global population. We refer to this function as $\text{FILTERANDEVAL}(C, \mathcal{T}, \mathcal{D}, \alpha)$ (Algorithm 3 and step 7 of Algorithm 1). Lastly, we add the remaining trainable models and their associated fitness scores into G

(step 8 of Algorithm 1).

Fitness-based selection   After evaluating all child models in the current round, we apply fitness-based selection to identify top candidate models for crossover (step 10 of Algorithm 1). We denote this as $\text{GETTOP}(G, p)$, which refers simply to selecting the p models with the highest fitness scores from G. Once these models have been selected, they are permanently removed from the population and cannot be used again as parents for crossover.

Training π_{θ_t}   Lastly, all child models generated in the current round that were not previously selected for crossover (*i.e.* $C_{\text{EVALED}} \setminus P$) are used to prompt-tune π_θ for the next round (step 11 of Algorithm 1).

4. Experiments and Results

We evaluate our meta-learning algorithm on two datasets - MNIST-1D (Greydanus, 2020) and the CLRS algorithmic reasoning benchmark (Veličković et al., 2022). While the former benchmark is lightweight and permits us to do a more thorough analysis of our algorithm, the latter is a newer benchmark with more headroom for discovering novel architectures with better performance.

In all of our experiments, our π_{θ_0} (*i.e.* the crossover operator) is a 62B parameter PALM model (Chowdhery et al., 2022) pre-trained on 1.3T tokens of conversational, web, and code documents. It is additionally fine-tuned on a corpus of 64B tokens from near-deduplicated, permissively-licensed Python source code files from Github. We always sample from π_{θ_0} with mixed temperature sampling, in which the sampling temperature is selected uniformly from $[0.2, 0.6, 0.8, 1.0]$. Between each round, the model is prompt-tuned (Lester et al., 2021) for 5 epochs with a soft prompt length of 16, batch size of 16, and learning rate of 0.1 (as described in Section 3.3 and Step 11 of Algorithm 1). Unless stated otherwise, we run 10 rounds of evolution with 10 prompts per round and 16 samples generated per prompt, yielding a total of 160 models generated per round and 1600 models generated during the entire search. Duplicate models and un-trainable models are not scored, but do count into the 1600. All other EVOPROMPTING hyperparameters are listed in Table A.1.

4.1. MNIST-1D

Dataset   We apply our method first to MNIST-1D (Greydanus, 2020), a one-dimensional, scaled-down version of the MNIST-1D dataset containing examples that are 20 times smaller than the original MNIST dataset. Each example is only 40-dimensional, with 4000 examples in the training dataset and 1000 in test. Since there is no validation dataset, we randomly set aside 500 examples from the train-

ing dataset to use as the validation dataset. Despite being more lightweight, MNIST-1D distinguishes more between different architecture types (Greydanus, 2020) than its larger counterpart MNIST (LeCun et al., 1998).

Meta-learning set-up   Throughout the model search we use the AdamW optimizer (Loshchilov & Hutter, 2019) to train each child model on a single NVIDIA Tesla P100 GPU for 8000 steps, with learning rate 0.01 and batch size 128. We score child models according to the best validation accuracy achieved during training.

We also seed the search with 4 seed models - the 3 hand-designed neural baselines from the original MNIST-1D paper (Greydanus, 2020) (GRU, CNN, and MLP) and a fourth, larger CNN model of our own design. All four are implemented with Flax (Heek et al., 2020). We refer the reader to Appendix A.2 for the source code of these seed models.

Baselines   We compare EVOPROMPTING with the following baselines:

- Naive few-shot prompting: This baseline simply generates code samples $c \sim \pi_{\theta_0}(\cdot|p)$, where p is a 2-shot prompt constructed using in-context examples randomly selected from the seed models (Listing 1). This is essentially an ablation of steps 7-12 in Algorithm 1 with $T = 1$. We increase the number of samples generated per prompt for the naive prompting baseline such that the total number of samples generated by π_θ matches that of the other baselines.

- EVOPROMPTING (- prompt-tuning): We run the entire algorithm as is, but without prompt-tuning between each round. This is an ablation of step 11 from Algorithm 1

- EVOPROMPTING (random parents): Instead of selecting the most fit models from the last round as parents for the next round, we select parents randomly. This is an ablation of Step 10 in Algorithm 1, which is the $\text{GETTOP}(G, p)$ step.

EVOPROMPTING finds smaller and more accurate models   Figure 1 shows a comparison of the test error and model size of the top 20 models discovered by EVOPROMPTING compared with those of our seed models and three baselines. The points approximate a Pareto frontier, below which each algorithm cannot improve on one dimension without hurting the other. EVOPROMPTING possesses the Pareto frontier closest to the origin, indicating that it finds more optimal models in terms of accuracy and size. In fact, many models in EVOPROMPTING's top 20 discovered models are orders of magnitude smaller than those of the other baselines, while still having lower test error.

We also note that – on this task in particular – EVOPROMPT-ING excels especially at optimizing convolutional architectures. Many of the top 20 models are narrower and deeper convolutional architectures, with smaller strides, less padding, and no dense layers. These models consistently perform better than the shallower, denser, and wider convolutional architectures seen in earlier rounds of the model search.
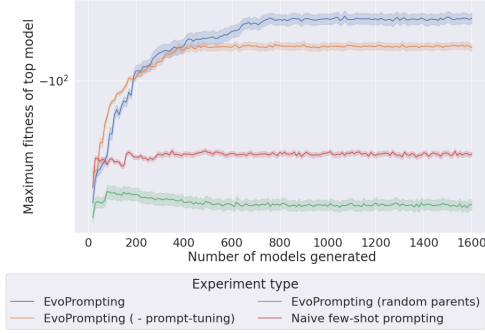

Figure 3. Number of child models generated versus maximum fitness in sample, as estimated using 100 bootstrap samples of size 20 for each point along the x-axis.

Another important aspect of a meta-learning algorithm is the relationship between the number of individuals evaluated and the maximum fitness observed so far, *i.e.* the sample efficiency. Neural architecture search can be an expensive process, with the most open-ended searches requiring the evaluation of trillions of individuals (Real et al., 2020). Thus, it is crucial to identify fit candidates using as few samples as possible. As such, we analyze the rate at which the fitness of the best-performing child model improves as a function of the number of child samples generated thus far, as shown in Figure 3. The random parents baseline plateaus the quickest, reaching a maximum fitness by the time approximately 200 individuals have been generated. Furthermore, the maximum fitness it reaches is significantly worse than that of the other experiments. On the other hand, EVOPROMPTING without prompt-tuning and normal EVOPROMPTING do not plateau until much later on. EVO-PROMPTING's plateau is the highest and therefore fitter on average than the individuals discovered by any of the other experiments.

It is also evident from both Figure 1 and 3 that performance suffers when any individual component is removed. Interestingly, Figure 1 indicates that prompting with randomly selected parents combined with prompt-tuning is no more effective than naive prompting alone. This highlights the importance of selecting helpful in-context examples, particularly in a task for which we assume that less training signal exists in the pre-training data. However, selecting more fit models as in-context examples without prompt-tuning also does not perform nearly as well as our full method.
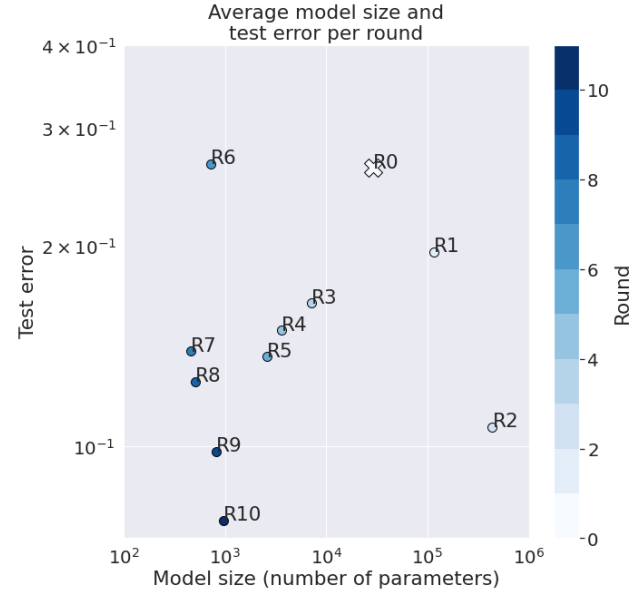

Figure 4. The average model size and test error of the child models produced in each round of the model search. Data points closer to the origin represent rounds that yielded more "fit" models.

Trajectory over meta-learning rounds We also explored the trajectory of our meta-learning algorithm round over round, as shown in Figure 4. In general, we observe that EVOPROMPTING starts out further away from the origin (in round 0) and ends up closest to the origin in round 10, which signifies that it discovers – on average – the smallest and most accurate models in the last round. However, the search does not always yield improvements on both axes between consecutive rounds. In rounds 0-2 and 6-10, EVO-PROMPTING improves test error while trading off model size. On the other hand, both dimensions are simultaneously improved upon in rounds 3-5.

4.2. CLRS

Although the MNIST-1D task offers an efficient and practical setting for evaluating a meta-learning algorithm, CNN architectures already perform fairly well on this task and neural image classification architectures have been extensively studied as a whole. There also exists the possibility that our LM has seen many convolutional architectures in its pre-training data. Instead, we turn to a different learning task and class of neural network architectures in order to assess whether our meta-learning framework generalizes to other tasks, datasets, and neural architectures.

Dataset The CLRS algorithmic reasoning benchmark (Veličković et al., 2022) evaluates the ability of neural networks to learn algorithmic reasoning across a set of 30 classical algorithms covered in the *Introduction to Algorithms*
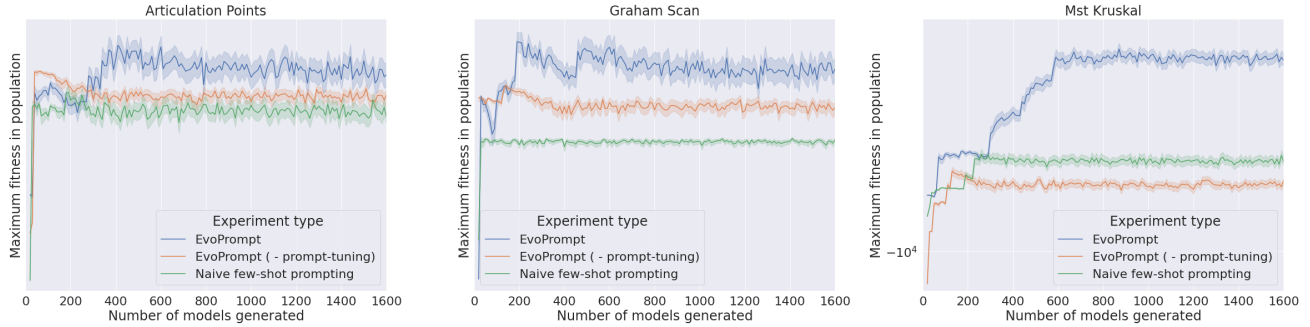
Figure 5. Number of child models generated versus maximum fitness of top model seen so far (as estimated using 100 bootstrap samples of size 20 for each point along the x-axis) when searching over neural network models for three CLRS tasks. As mentioned in Section 4.2, these algorithms were selected because our preliminary analyses indicated that they had the most headroom for architectural improvements.

textbook by Cormen, Leiserson, Rivest and Stein (Cormen et al., 2009). This benchmark is useful not only as a difficult logical reasoning task for neural networks, but also as a measure of a neural network's *algorithmic alignment* (Xu et al., 2020). In brief, algorithmic alignment refers to a model's ability to reason like an algorithm (*i.e.* using the computation graph for a task), rather than relying upon memorization or other less sample efficient learning strategies. Although a model can approximate an algorithm by pattern-matching against similar inputs or relying on other shortcuts, it cannot generalize to arbitrarily long inputs or edge cases without learning the computation graph underlying the algorithm.

Accordingly, the CLRS benchmark represents the algorithms' inputs and outputs as graphs, and the steps of the algorithm as a *trajectory* of operations over the input graph. This problem setup can be straightforwardly processed by graph neural networks, which is explored in Ibarz et al. (2022). They find that a Triplet-GMPNN model (a message-passing neural network (Gilmer et al., 2017) with gating and triplet edge processing) exhibits the best performance when trained and evaluated across all 30 algorithms at once.

Meta-learning set-up   Similar to our MNIST-1D set-up, we use the AdamW optimizer to train each child model on a single NVIDIA Tesla P100 GPU. However, since most of the explored child models were much larger than the MNIST-1D models, we only trained each child model for 2000 steps. Anecdotally, we observed that the performance of different models often diverged by 2000 steps, which provided sufficient signal for the model search process. We otherwise followed the hyperparameters for single-task training in Ibarz et al. (2022) and evaluated models using validation accuracy.

Unlike our MNIST-1D set-up, we only search over the triplet representations of a Triplet-GMPNN model (see Ibarz et al. (2022) for more details), rather than the entire graph processor. We also seed the search with nine different seed models - each a variant of a Triplet-GMPNN model with a different

triplet representation. Each seed triplet representation incorporates a minor tweak of a single component of the original triplet representation designed by Ibarz et al. (2022). These include a fully-connected output layer, a sum aggregation, fully-connected node/edge/graph representations, a simple linear triplet representation, and a bilinear representation (Mnih & Hinton, 2007). All nine are implemented with Haiku (Hennigan et al., 2020), an object-oriented neural network library for Jax (see Appendix A.4 for the source code of the seed models.)

Generalizing beyond image classification models   We search using EVOPROMPTING on 3 individual algorithms in the CLRS benchmark – the articulation points, Graham scan, and Kruskal's minimum spanning tree algorithms. We select these algorithms because our preliminary analyses with hand-designed architectures showed that they had the most headroom for improvement, although we found that the discovered architectures transfer well to other CLRS benchmark tasks as well (Appx. A.5). Our search results are shown in Figure 5. EVOPROMPTING continues to find models that are more "fit" than our other two baselines, though we observed that the results also show more variation than our results for MNIST-1D did.

Analyzing newly discovered models   Our search across triplet representations yielded several new designs that we sought to evaluate across all algorithms in the CLRS benchmark. Although these new models were discovered in model searches over single algorithms, they oftentimes generalized to other algorithms that were unseen during the model search. Figure 6 shows the trajectory of validation accuracy during training and Table 4.2 provides OOD accuracies for these models on a few select algorithms. (We defer the reader to Appendix A.3 for the full source code of each newly discovered model and Table A.5 for the full list of OOD accuracies for every algorithm in the CLRS benchmark.)

We note that the model search suggested several simple

Table 1. A comparison of OOD accuracy and model size (in number of parameters) of models newly discovered by EVOPROMPTING on select CLRS tasks where EVOPROMPTING has discovered more accurate architectures without large increases in model size, compared with the baseline model (the Triplet-GMPNN from Ibarz et al. (2022)). OOD accuracy numbers for the baseline model are from Ibarz et al. (2022). For the full table of results on all CLRS tasks, including accuracies of our own implementation of the Triplet-GMPNN, see Appendix A.5.

CLRS task	Best performing model	Model Size ↓			OOD accuracy ↑		
		Ours	Baseline	% Change	Ours	Baseline	% Change
Articulation Points	QUADNODEMINMAX	497969	531913	-6.38%	**93.46 ± 1.77%**	88.32± 2.01%	5.82%
BFS	MAXMEAN	522931	523963	-0.20%	**99.99 ± 0.01%**	99.73± 0.04%	0.26%
Bubble Sort	CONCATREP	568533	524477	8.40%	**88.87 ± 2.77%**	67.68± 5.50%	31.31%
DFS	DIV2MEAN	660158	661190	-0.16%	**68.14 ± 1.38%**	47.79± 4.19%	42.58%
Floyd Warshall	CONCATREP	669145	625089	7.05%	**61.43 ± 0.79%**	48.52± 1.04%	26.61%
Heapsort	CONCATREP	703710	659654	6.68%	**69.90 ± 4.17%**	31.04± 5.82%	125.19%
Insertion Sort	DIV2MEAN	523445	524477	-0.20%	**89.47 ± 2.57%**	78.14± 4.64%	14.50%
Quicksort	DIV2MEAN	524727	525759	-0.20%	**85.23 ± 4.26%**	64.64± 5.12%	31.85%
Task Scheduling	TANHEXPANDTRIPLETS	262333	262333	0.00%	**88.23 ± 0.44%**	87.25± 0.35%	1.12%

but effective changes. For example, instead of taking the maximum of the triplet representation, the QUADNODEM-INMAX model uses quadruplet node representations instead of triplets, and it subtracts the minimum of the quad representation from the max instead. CONCATREP represents the node, edge, and graph representations as a concatenation of a projection feedforward layer, and MAXMEAN takes the maximum of the triplet representations prior to taking the mean and passing it through the output dense layer. DIV2MEAN scales each of the node representations by $1/2$ and uses a mean aggregation of the triplet representations instead of the max aggregation. TANHEXPANDTRIPLETS applies additional dimension expansion to the triplet representations and applies a hyperbolic tangent function after the max aggregation. See Appx. A.3 for the full code of each discovered model.

Of the 5 newly discovered models that we chose to analyze, CONCATREP is the only one that increases model size. However, as shown in Table 4.2, CONCATREP frequently yielded improvements in OOD accuracy that far exceeded the percent increase in model size. For instance, on the heapsort algorithm CONCATREP increased OOD accuracy by 125.19% while only increasing model size by 6.68% over the baseline. The other four newly discovered models shown in Table 4.2 simultaneously improved OOD accuracy while decreasing model size on the articulation points, BFS, DFS, insertion sort, quicksort, and task scheduling algorithms. On the rest of the CLRS algorithms (Table A.5), our newly discovered models typically achieved OOD accuracy comparable to or better than the baseline, while maintaining similar model size.

5. Conclusion

We have shown that embedding a pre-trained LM in an evolutionary algorithm significantly improves the LM's performance on the task of neural architecture design. Our approach has demonstrated success at not only optimizing convolutional architectures for the MNIST-1D task, but also at developing new kinds of GNNs for the CLRS algorithmic benchmark. This demonstrates: 1) using evolutionary techniques can vastly improve the few-shot/in-context capabilities of pre-trained LMs, and 2) EVOPROMPTING can discover novel, competitive, and even state-of-the-art architectures that optimize for both accuracy and model size. Furthermore, EVOPROMPTING is general enough to be easily adapted to search for solutions to other kinds of reasoning tasks beyond NAS.

However, this study has its limitations. Firstly, we have not compared to typical NAS methods, as these require manually designed search spaces – a confounder that prevents fair comparison on these tasks if we designed these spaces ourselves. Secondly, our study has been orders of magnitudes smaller than previous works in terms of compute. Future work could scale up our approach to compare against more competitive large-scale architectures, such as Transformers.

6. Acknowledgements

References

Ahmad, W. U., Chakraborty, S., Ray, B., and Chang, K.-W. Unified pre-training for program understanding and generation. *ArXiv*, abs/2103.06333, 2021.

Bender, G., Liu, H., Chen, B., Chu, G., Cheng, S., Kindermans, P.-J., and Le, Q. V. Can weight sharing outperform random architecture search? an investigation with tunas. *2020 IEEE/CVF Conference on Computer Vision and Pattern Recognition (CVPR)*, pp. 14311–14320, 2020.

BigScience Workshop, :, Scao, T. L., Fan, A., Akiki, C., Pavlick, E., Ilić, S., Hesslow, D., Castagné, R., Luccioni, A. S., Yvon, F., Gallé, M., Tow, J., Rush, A. M., Biderman, S., Webson, A., Ammanamanchi, P. S., Wang, T., Sagot, B., Muennighoff, N., del Moral, A. V., Ruwase, O., Bawden, R., Bekman, S., McMillan-Major, A., Beltagy, I., Nguyen, H., Saulnier, L., Tan, S., Suarez, P. O., Sanh, V., Laurençon, H., Jernite, Y., Launay, J., Mitchell, M., Raffel, C., Gokaslan, A., Simhi, A., Soroa, A., Aji, A. F., Alfassy, A., Rogers, A., Nitzav, A. K., Xu, C., Mou, C., Emezue, C., Klamm, C., Leong, C., van Strien, D., Adelani, D. I., Radev, D., Ponferrada, E. G., Levkovizh, E., Kim, E., Natan, E. B., De Toni, F., Dupont, G., Kruszewski, G., Pistilli, G., Elsahar, H., Benyamina, H., Tran, H., Yu, I., Abdulmumin, I., Johnson, I., Gonzalez-Dios, I., de la Rosa, J., Chim, J., Dodge, J., Zhu, J., Chang, J., Frohberg, J., Tobing, J., Bhattacharjee, J., Almubarak, K., Chen, K., Lo, K., Von Werra, L., Weber, L., Phan, L., allal, L. B., Tanguy, L., Dey, M., Muñoz, M. R., Masoud, M., Grandury, M., Šaško, M., Huang, M., Coavoux, M., Singh, M., Jiang, M. T.-J., Vu, M. C., Jauhar, M. A., Ghaleb, M., Subramani, N., Kassner, N., Khamis, N., Nguyen, O., Espejel, O., de Gibert, O., Villegas, P., Henderson, P., Colombo, P., Amuok, P., Lhoest, Q., Harliman, R., Bommasani, R., López, R. L., Ribeiro, R., Osei, S., Pyysalo, S., Nagel, S., Bose, S., Muhammad, S. H., Sharma, S., Longpre, S., Nikpoor, S., Silberberg, S., Pai, S., Zink, S., Torrent, T. T., Schick, T., Thrush, T., Danchev, V., Nikoulina, V., Laippala, V., Lepercq, V., Prabhu, V., Alyafeai, Z., Talat, Z., Raja, A., Heinzerling, B., Si, C., Taşar, D. E., Salesky, E., Mielke, S. J., Lee, W. Y., Sharma, A., Santilli, A., Chaffin, A., Stiegler, A., Datta, D., Szczechla, E., Chhablani, G., Wang, H., Pandey, H., Strobelt, H., Fries, J. A., Rozen, J., Gao, L., Sutawika, L., Bari, M. S., Al-shaibani, M. S., Manica, M., Nayak, N., Teehan, R., Albanie, S., Shen, S., Ben-David, S., Bach, S. H., Kim, T., Bers, T., Fevry, T., Neeraj, T., Thakker, U., Raunak, V., Tang, X., Yong, Z.-X., Sun, Z., Brody, S., Uri, Y., Tojarieh, H., Roberts, A., Chung, H. W., Tae, J., Phang, J., Press, O., Li, C., Narayanan, D., Bourfoune, H., Casper, J., Rasley, J., Ryabinin, M., Mishra, M., Zhang, M., Shoeybi, M., Peyrounette, M., Patry, N., Tazi, N., Sanseviero, O., von Platen, P., Cornette, P., Lavallée, P. F., Lacroix, R., Rajbhandari, S., Gandhi, S., Smith, S., Requena, S., Patil, S., Dettmers, T., Baruwa, A., Singh, A., Cheveleva, A., Ligozat, A.-L., Subramonian, A., Névéol, A., Lovering, C., Garrette, D., Tunuguntla, D., Reiter, E., Taktasheva, E., Voloshina, E., Bogdanov, E., Winata, G. I., Schoelkopf, H., Kalo, J.-C., Novikova, J., Forde, J. Z., Clive, J., Kasai, J., Kawamura, K., Hazan, L., Carpuat, M., Clinciu, M., Kim, N., Cheng, N., Serikov, O., Antverg, O., van der Wal, O., Zhang, R., Zhang, R., Gehrmann, S., Mirkin, S., Pais, S., Shavrina, T., Scialom, T., Yun, T., Limisiewicz, T., Rieser, V., Protasov, V., Mikhailov, V., Pruksachatkun, Y., Belinkov, Y., Bamberger, Z., Kasner, Z., Rueda, A., Pestana, A., Feizpour, A., Khan, A., Faranak, A., Santos, A., Hevia, A., Unldreaj, A., Aghagol, A., Abdollahi, A., Tammour, A., HajiHosseini, A., Behroozi, B., Ajibade, B., Saxena, B., Ferrandis, C. M., Contractor, D., Lansky, D., David, D., Kiela, D., Nguyen, D. A., Tan, E., Baylor, E., Ozoani, E., Mirza, F., Ononiwu, F., Rezanejad, H., Jones, H., Bhattacharya, I., Solaiman, I., Sedenko, I., Nejadgholi, I., Passmore, J., Seltzer, J., Sanz, J. B., Dutra, L., Samagaio, M., Elbadri, M., Mieskes, M., Gerchick, M., Akinlolu, M., McKenna, M., Qiu, M., Ghauri, M., Burynok, M., Abrar, N., Rajani, N., Elkott, N., Fahmy, N., Samuel, O., An, R., Kromann, R., Hao, R., Alizadeh, S., Shubber, S., Wang, S., Roy, S., Viguier, S., Le, T., Oyebade, T., Le, T., Yang, Y., Nguyen, Z., Kashyap, A. R., Palasciano, A., Callahan, A., Shukla, A., Miranda-Escalada, A., Singh, A., Beilharz, B., Wang, B., Brito, C., Zhou, C., Jain, C., Xu, C., Fourrier, C., Periñán, D. L., Molano, D., Yu, D., Manjavacas, E., Barth, F., Fuhrimann, F., Altay, G., Bayrak, G., Burns, G., Vrabec, H. U., Bello, I., Dash, I., Kang, J., Giorgi, J., Golde, J., Posada, J. D., Sivaraman, K. R., Bulchandani, L., Liu, L., Shinzato, L., de Bykhovetz, M. H., Takeuchi, M., Pàmies, M., Castillo, M. A., Nezhurina, M., Sänger, M., Samwald, M., Cullan, M., Weinberg, M., De Wolf, M., Mihaljcic, M., Liu, M., Freidank, M., Kang, M., Seelam, N., Dahlberg, N., Broad, N. M., Muellner, N., Fung, P., Haller, P., Chandrasekhar, R., Eisenberg, R., Martin, R., Canalli, R., Su, R., Su, R., Cahyawijaya, S., Garda, S., Deshmukh, S. S., Mishra, S., Kiblawi, S., Ott, S., Sang-aroonsiri, S., Kumar, S., Schweter, S., Bharati, S., Laud, T., Gigant, T., Kainuma, T., Kusa, W., Labrak, Y., Bajaj, Y. S., Venkatraman, Y., Xu, Y., Xu, Y., Xu, Y., Tan, Z., Xie, Z., Ye, Z., Bras, M., Belkada, Y., and Wolf, T. Bloom: A 176b-parameter open-access multilingual language model, 2022. URL https://arxiv.org/abs/2211.05100.

Brooks, E., Walls, L., Lewis, R. L., and Singh, S. In-context policy iteration, 2022. URL https://arxiv.org/abs/2210.03821.

Brown, T. B., Mann, B., Ryder, N., Subbiah, M., Kaplan, J., Dhariwal, P., Neelakantan, A., Shyam, P., Sastry, G.,

Askell, A., Agarwal, S., Herbert-Voss, A., Krueger, G., Henighan, T., Child, R., Ramesh, A., Ziegler, D. M., Wu, J., Winter, C., Hesse, C., Chen, M., Sigler, E., Litwin, M., Gray, S., Chess, B., Clark, J., Berner, C., McCandlish, S., Radford, A., Sutskever, I., and Amodei, D. Language models are few-shot learners, 2020. URL https://arxiv.org/abs/2005.14165.

Chen, M., Tworek, J., Jun, H., Yuan, Q., Ponde, H., Kaplan, J., Edwards, H., Burda, Y., Joseph, N., Brockman, G., Ray, A., Puri, R., Krueger, G., Petrov, M., Khlaaf, H., Sastry, G., Mishkin, P., Chan, B., Gray, S., Ryder, N., Pavlov, M., Power, A., Kaiser, L., Bavarian, M., Winter, C., Tillet, P., Such, F. P., Cummings, D. W., Plappert, M., Chantzis, F., Barnes, E., Herbert-Voss, A., Guss, W. H., Nichol, A., Babuschkin, I., Balaji, S. A., Jain, S., Carr, A., Leike, J., Achiam, J., Misra, V., Morikawa, E., Radford, A., Knight, M. M., Brundage, M., Murati, M., Mayer, K., Welinder, P., McGrew, B., Amodei, D., McCandlish, S., Sutskever, I., and Zaremba, W. Evaluating large language models trained on code. *ArXiv*, abs/2107.03374, 2021.

Chen, Y., Song, X., Lee, C., Wang, Z., Zhang, Q., Dohan, D., Kawakami, K., Kochanski, G., Doucet, A., Ranzato, M., Perel, S., and de Freitas, N. Towards learning universal hyperparameter optimizers with transformers, 2022. URL https://arxiv.org/abs/2205.13320.

Chowdhery, A., Narang, S., Devlin, J., Bosma, M., Mishra, G., Roberts, A., Barham, P., Chung, H. W., Sutton, C., Gehrmann, S., Schuh, P., Shi, K., Tsvyashchenko, S., Maynez, J., Rao, A., Barnes, P., Tay, Y., Shazeer, N., Prabhakaran, V., Reif, E., Du, N., Hutchinson, B., Pope, R., Bradbury, J., Austin, J., Isard, M., Gur-Ari, G., Yin, P., Duke, T., Levskaya, A., Ghemawat, S., Dev, S., Michalewski, H., Garcia, X., Misra, V., Robinson, K., Fedus, L., Zhou, D., Ippolito, D., Luan, D., Lim, H., Zoph, B., Spiridonov, A., Sepassi, R., Dohan, D., Agrawal, S., Omernick, M., Dai, A. M., Pillai, T. S., Pellat, M., Lewkowycz, A., Moreira, E., Child, R., Polozov, O., Lee, K., Zhou, Z., Wang, X., Saeta, B., Diaz, M., Firat, O., Catasta, M., Wei, J., Meier-Hellstern, K., Eck, D., Dean, J., Petrov, S., and Fiedel, N. Palm: Scaling language modeling with pathways, 2022. URL https://arxiv.org/abs/2204.02311.

Cormen, T. H., Leiserson, C. E., Rivest, R. L., and Stein, C. *Introduction to Algorithms, Third Edition*. The MIT Press, 3rd edition, 2009. ISBN 0262033844.

Dakhel, A. M., Majdinasab, V., Nikanjam, A., Khomh, F., Desmarais, M. C., and Jiang, Z. M. Github copilot ai pair programmer: Asset or liability? *ArXiv*, abs/2206.15331, 2022.

Dohan, D., Xu, W., Lewkowycz, A., Austin, J., Bieber, D., Lopes, R. G., Wu, Y., Michalewski, H., Saurous, R. A.,

Sohl-dickstein, J., Murphy, K., and Sutton, C. Language model cascades, 2022. URL https://arxiv.org/abs/2207.10342.

Du, N., Huang, Y., Dai, A. M., Tong, S., Lepikhin, D., Xu, Y., Krikun, M., Zhou, Y., Yu, A. W., Firat, O., Zoph, B., Fedus, L., Bosma, M., Zhou, Z., Wang, T., Wang, Y. E., Webster, K., Pellat, M., Robinson, K., Meier-Hellstern, K., Duke, T., Dixon, L., Zhang, K., Le, Q. V., Wu, Y., Chen, Z., and Cui, C. Glam: Efficient scaling of language models with mixture-of-experts, 2021. URL https://arxiv.org/abs/2112.06905.

Elsken, T., Metzen, J. H., and Hutter, F. Efficient multi-objective neural architecture search via lamarckian evolution. *arXiv: Machine Learning*, 2018.

Feng, Z., Guo, D., Tang, D., Duan, N., Feng, X., Gong, M., Shou, L., Qin, B., Liu, T., Jiang, D., and Zhou, M. Codebert: A pre-trained model for programming and natural languages. *ArXiv*, abs/2002.08155, 2020.

Gilmer, J., Schoenholz, S. S., Riley, P. F., Vinyals, O., and Dahl, G. E. Neural message passing for quantum chemistry. In *Proceedings of the 34th International Conference on Machine Learning - Volume 70*, ICML'17, pp. 1263–1272. JMLR.org, 2017.

Greydanus, S. Scaling *down* deep learning. *CoRR*, abs/2011.14439, 2020. URL https://arxiv.org/abs/2011.14439.

Heek, J., Levskaya, A., Oliver, A., Ritter, M., Rondepierre, B., Steiner, A., and van Zee, M. Flax: A neural network library and ecosystem for JAX, 2020. URL http://github.com/google/flax.

Hennigan, T., Cai, T., Norman, T., and Babuschkin, I. Haiku: Sonnet for JAX, 2020. URL http://github.com/deepmind/dm-haiku.

Ibarz, B., Kurin, V., Papamakarios, G., Nikiforou, K., Bennani, M. A., Csordás, R., Dudzik, A., Bovsnjak, M., Vitvitskyi, A., Rubanova, Y., Deac, A., Bevilacqua, B., Ganin, Y., Blundell, C., and Veličković, P. A generalist neural algorithmic learner. *ArXiv*, abs/2209.11142, 2022.

Kojima, T., Gu, S. S., Reid, M., Matsuo, Y., and Iwasawa, Y. Large language models are zero-shot reasoners. *ArXiv*, abs/2205.11916, 2022.

Koza, J. R. Genetic programming - on the programming of computers by means of natural selection. In *Complex Adaptive Systems*, 1993.

Kudo, T. and Richardson, J. Sentencepiece: A simple and language independent subword tokenizer and detokenizer for neural text processing. In *Conference on Empirical Methods in Natural Language Processing*, 2018.

LeCun, Y., Bottou, L., Bengio, Y., and Haffner, P. Gradient-based learning applied to document recognition. *Proc. IEEE*, 86:2278–2324, 1998.

Lehman, J., Gordon, J., Jain, S., Ndousse, K., Yeh, C., and Stanley, K. O. Evolution through large models. *ArXiv*, abs/2206.08896, 2022.

Lester, B., Al-Rfou, R., and Constant, N. The power of scale for parameter-efficient prompt tuning, 2021. URL https://arxiv.org/abs/2104.08691.

Li, L. and Talwalkar, A. S. Random search and reproducibility for neural architecture search. *ArXiv*, abs/1902.07638, 2019.

Liu, H., Brock, A., Simonyan, K., and Le, Q. V. Evolving normalization-activation layers. *ArXiv*, abs/2004.02967, 2020.

Liu, J., Shen, D., Zhang, Y., Dolan, B., Carin, L., and Chen, W. What makes good in-context examples for gpt-3? In *Workshop on Knowledge Extraction and Integration for Deep Learning Architectures; Deep Learning Inside Out*, 2021.

Loshchilov, I. and Hutter, F. Decoupled weight decay regularization. In *International Conference on Learning Representations*, 2019. URL https://openreview.net/forum?id=Bkg6RiCqY7.

Lu, Y., Bartolo, M., Moore, A., Riedel, S., and Stenetorp, P. Fantastically ordered prompts and where to find them: Overcoming few-shot prompt order sensitivity. In *Annual Meeting of the Association for Computational Linguistics*, 2021.

Meyerson, E., Nelson, M. J., Bradley, H., Moradi, A., Hoover, A. K., and Lehman, J. Language model crossover: Variation through few-shot prompting, 2023. URL https://arxiv.org/abs/2302.12170.

Min, S., Lyu, X., Holtzman, A., Artetxe, M., Lewis, M., Hajishirzi, H., and Zettlemoyer, L. Rethinking the role of demonstrations: What makes in-context learning work? *ArXiv*, abs/2202.12837, 2022.

Mnih, A. and Hinton, G. Three new graphical models for statistical language modelling. In *Proceedings of the 24th International Conference on Machine Learning*, ICML '07, pp. 641–648, New York, NY, USA, 2007. Association for Computing Machinery. ISBN 9781595937933. doi: 10.1145/1273496.1273577. URL https://doi.org/10.1145/1273496.1273577.

Noorbakhsh, K., Sulaiman, M., Sharifi, M., Roy, K., and Jamshidi, P. Pretrained language models are symbolic mathematics solvers too! *ArXiv*, abs/2110.03501, 2021.

Odena, A., Sutton, C., Dohan, D. M., Jiang, E., Michalewski, H., Austin, J., Bosma, M. P., Nye, M., Terry, M., and Le, Q. V. Program synthesis with large language models. In *n/a*, pp. n/a, n/a, 2021. n/a.

Ouyang, L., Wu, J., Jiang, X., Almeida, D., Wainwright, C. L., Mishkin, P., Zhang, C., Agarwal, S., Slama, K., Ray, A., Schulman, J., Hilton, J., Kelton, F., Miller, L. E., Simens, M., Askell, A., Welinder, P., Christiano, P. F., Leike, J., and Lowe, R. J. Training language models to follow instructions with human feedback. *ArXiv*, abs/2203.02155, 2022.

Qian, J., Wang, H., Li, Z., LI, S., and Yan, X. Limitations of language models in arithmetic and symbolic induction. *ArXiv*, abs/2208.05051, 2022.

Real, E., Moore, S., Selle, A., Saxena, S., Suematsu, Y. L., Tan, J., Le, Q. V., and Kurakin, A. Large-scale evolution of image classifiers. *ArXiv*, abs/1703.01041, 2017.

Real, E., Aggarwal, A., Huang, Y., and Le, Q. V. Regularized evolution for image classifier architecture search. In *AAAI Conference on Artificial Intelligence*, 2018.

Real, E., Liang, C., So, D. R., and Le, Q. V. Automl-zero: Evolving machine learning algorithms from scratch. In *International Conference on Machine Learning*, 2020.

Rubin, O., Herzig, J., and Berant, J. Learning to retrieve prompts for in-context learning. *ArXiv*, abs/2112.08633, 2021.

Sanh, V., Webson, A., Raffel, C., Bach, S. H., Sutawika, L., Alyafeai, Z., Chaffin, A., Stiegler, A., Scao, T. L., Raja, A., Dey, M., Bari, M. S., Xu, C., Thakker, U., Sharma, S., Szczechla, E., Kim, T., Chhablani, G., Nayak, N. V., Datta, D., Chang, J., Jiang, M. T.-J., Wang, H., Manica, M., Shen, S., Yong, Z. X., Pandey, H., Bawden, R., Wang, T., Neeraj, T., Rozen, J., Sharma, A., Santilli, A., Févry, T., Fries, J. A., Teehan, R., Biderman, S. R., Gao, L., Bers, T., Wolf, T., and Rush, A. M. Multitask prompted training enables zero-shot task generalization. *ArXiv*, abs/2110.08207, 2021.

Sciuto, C., Yu, K., Jaggi, M., Musat, C. C., and Salzmann, M. Evaluating the search phase of neural architecture search. *ArXiv*, abs/1902.08142, 2019.

So, D. R., Liang, C., and Le, Q. V. The evolved transformer. *ArXiv*, abs/1901.11117, 2019.

So, D. R., Mańke, W., Liu, H., Dai, Z., Shazeer, N., and Le, Q. V. Primer: Searching for efficient transformers for language modeling, 2021. URL https://arxiv.org/abs/2109.08668.

Thoppilan, R., De Freitas, D., Hall, J., Shazeer, N., Kulshreshtha, A., Cheng, H.-T., Jin, A., Bos, T., Baker, L., Du, Y., Li, Y., Lee, H., Zheng, H. S., Ghafouri, A., Menegali, M., Huang, Y., Krikun, M., Lepikhin, D., Qin, J., Chen, D., Xu, Y., Chen, Z., Roberts, A., Bosma, M., Zhao, V., Zhou, Y., Chang, C.-C., Krivokon, I., Rusch, W., Pickett, M., Srinivasan, P., Man, L., Meier-Hellstern, K., Morris, M. R., Doshi, T., Santos, R. D., Duke, T., Soraker, J., Zevenbergen, B., Prabhakaran, V., Diaz, M., Hutchinson, B., Olson, K., Molina, A., Hoffman-John, E., Lee, J., Aroyo, L., Rajakumar, R., Butryna, A., Lamm, M., Kuzmina, V., Fenton, J., Cohen, A., Bernstein, R., Kurzweil, R., Aguera-Arcas, B., Cui, C., Croak, M., Chi, E., and Le, Q. Lamda: Language models for dialog applications, 2022. URL https://arxiv.org/abs/2201.08239.

Vaswani, A., Shazeer, N., Parmar, N., Uszkoreit, J., Jones, L., Gomez, A. N., Kaiser, L., and Polosukhin, I. Attention is all you need, 2017. URL https://arxiv.org/abs/1706.03762.

Veličković, P., Badia, A. P., Budden, D., Pascanu, R., Banino, A., Dashevskiy, M., Hadsell, R., and Blundell, C. The clrs algorithmic reasoning benchmark. In *International Conference on Machine Learning*, 2022.

Wang, Y., Wang, W., Joty, S. R., and Hoi, S. C. H. Codet5: Identifier-aware unified pre-trained encoder-decoder models for code understanding and generation. *ArXiv*, abs/2109.00859, 2021.

Wei, J., Bosma, M., Zhao, V., Guu, K., Yu, A. W., Lester, B., Du, N., Dai, A. M., and Le, Q. V. Finetuned language models are zero-shot learners. *ArXiv*, abs/2109.01652, 2021.

Wei, J., Wang, X., Schuurmans, D., Bosma, M., hsin Chi, E. H., Le, Q., and Zhou, D. Chain of thought prompting elicits reasoning in large language models. *ArXiv*, abs/2201.11903, 2022.

Xu, F. F., Alon, U., Neubig, G., and Hellendoorn, V. J. A systematic evaluation of large language models of code. *Proceedings of the 6th ACM SIGPLAN International Symposium on Machine Programming*, 2022.

Xu, K., Li, J., Zhang, M., Du, S. S., ichi Kawarabayashi, K., and Jegelka, S. What can neural networks reason about? In *International Conference on Learning Representations*, 2020. URL https://openreview.net/forum?id=rJxbJeHFPS.

Yao, X. Evolving artificial neural networks. *Proc. IEEE*, 87: 1423–1447, 1999.

Zhang, S., Roller, S., Goyal, N., Artetxe, M., Chen, M., Chen, S., Dewan, C., Diab, M., Li, X., Lin, X. V., Mihaylov, T., Ott, M., Shleifer, S., Shuster, K., Simig, D., Koura, P. S., Sridhar, A., Wang, T., and Zettlemoyer, L. Opt: Open pre-trained transformer language models, 2022. URL https://arxiv.org/abs/2205.01068.

Zhao, T., Wallace, E., Feng, S., Klein, D., and Singh, S. Calibrate before use: Improving few-shot performance of language models. *ArXiv*, abs/2102.09690, 2021.

Zhou, Y., Muresanu, A. I., Han, Z., Paster, K., Pitis, S., Chan, H., and Ba, J. Large language models are human-level prompt engineers. *ArXiv*, abs/2211.01910, 2022.

Zoph, B. and Le, Q. V. Neural architecture search with reinforcement learning, 2016. URL https://arxiv.org/abs/1611.01578.

A. Appendix

A.1. EVOPROMPTING Hyperparameters

Table 2. Values of hyperparameters used in EVOPROMPT.

HYPERPARAMETER	DESCRIPTION	VALUE
p	Num. parents to select in every generation	10
k	Num. in-context examples in prompt	2
T	Num. rounds of evolution	10
m	Num. prompts per round	10
n	Num. samples to generate per prompt	16
α	Lower threshold for test error	0.5

A.2. MNIST-1D Seed Models

Below we provide the source code for the four seed models used in the MNIST-1D model search.

```python
class Model(nn.Module):
  features: int = 32
  nlayer: int = 3

  @nn.compact
  def __call__(self, x):
    x = x[..., None]
    x = nn.Conv(features=self.features, kernel_size=(3,))(x)
    x = nn.relu(x)

    x = nn.avg_pool(x, window_shape=(2,), strides=(2,))
    for _ in range(self.nlayer - 1):
      xp = nn.Conv(
          features=self.features,
          kernel_size=(3,),
      )(x)
      xp = nn.relu(xp)
      x = x + xp

    x = nn.avg_pool(x, window_shape=(2,), strides=(2,))
    x = x.reshape((x.shape[0], -1))  # flatten
    x = nn.Dense(features=256)(x)
    x = nn.relu(x)
    x = nn.Dense(features=10)(x)
    return x
```

Listing 2. A hand-designed convolutional model.

```python
class Model(nn.Module):
  features: int = 25

  @nn.compact
  def __call__(self, x):
    x = x[..., None]
    x = nn.Conv(
        features=self.features, kernel_size=(5,), strides=(2,), padding=(1,)
    )(x)
    x = nn.relu(x)
    for _ in range(2):
      x = nn.Conv(
          features=self.features, kernel_size=(3,), strides=(2,), padding=(1,)
```

```
14          )(x)
15        x = nn.relu(x)
16      x = x.reshape((x.shape[0], -1))
17      x = nn.Dense(features=10)(x)
18      return x
```

Listing 3. A Flax implementation of the convolutional baseline from Greydanus (2020).

```
1  class Model(nn.Module):
2    """A simple GRU model."""
3
4    hidden_size: int = 6
5    seed: int = 42
6
7    @nn.compact
8    def __call__(self, x):
9      x = jnp.expand_dims(x, -1)
10     rng = jax_random.PRNGKey(self.seed)
11     gru = recurrent.GRU(
12         hidden_size=self.hidden_size,
13         num_layers=1,
14         dropout_rate=0.0,
15         bidirectional=True,
16     )
17     lengths = np.full([x.shape[0]], x.shape[1])
18     initialized_params = gru.init(rng, x, lengths)
19     params = initialized_params['params']
20     outputs, _ = gru.apply({'params': params}, x, lengths)
21     outputs = outputs.reshape((outputs.shape[0], -1))
22     x = nn.Dense(features=10)(outputs)
23     return x
```

Listing 4. A Flax implementation of the GRU baseline from Greydanus (2020).

```
1  class Model(nn.Module):
2    hidden_size: int = 100
3
4    @nn.compact
5    def __call__(self, x):
6      x = nn.Dense(features=self.hidden_size)(x)
7      x = nn.relu(x)
8      x = x + nn.relu(nn.Dense(features=self.hidden_size)(x))
9      x = nn.Dense(features=10)(x)
10     return x
11
12 return Model
```

Listing 5. A Flax implementation of the fully connected baseline from Greydanus (2020).
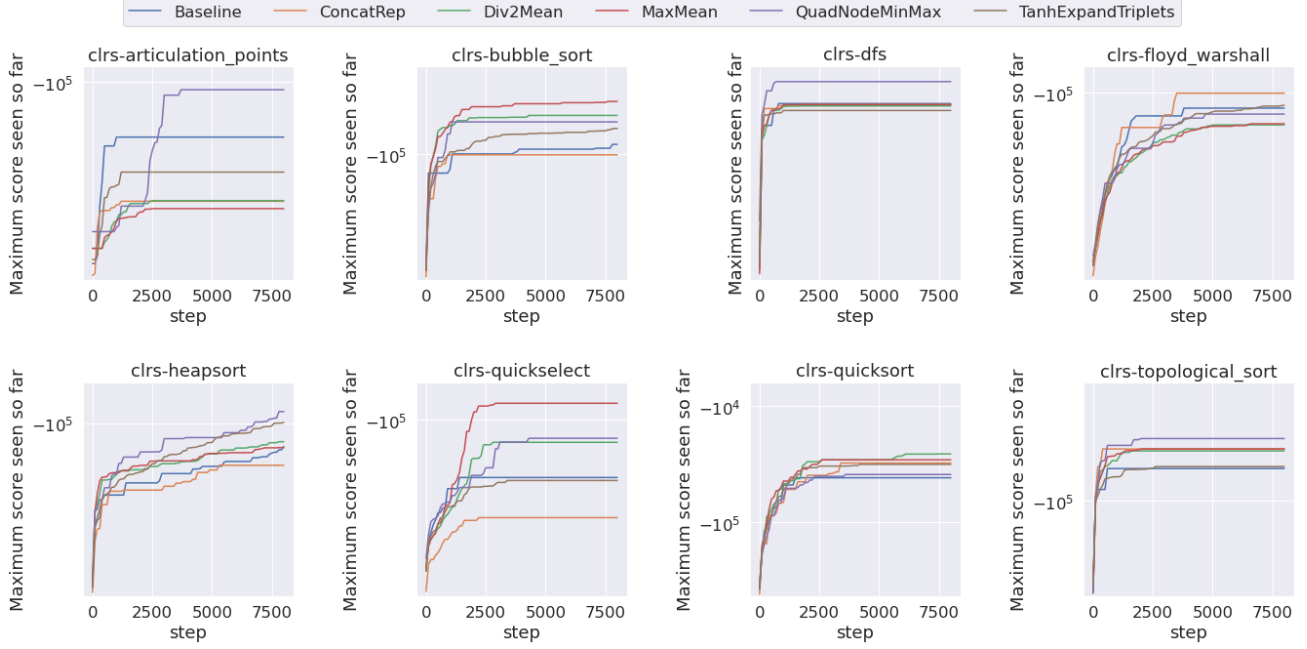
A.3. Newly Discovered CLRS GNNs

Figure 6. Maximum fitness scores of five of the newly discovered models, compared against the baseline, on eight of the CLRS tasks.

Below we list the Python source code of five of the newly discovered GNNs.

```python
def get_triplet_msgs_quad(z, edge_fts, graph_fts, nb_triplet_fts, out_size):
    node_reps = [hk.Linear(nb_triplet_fts) for _ in range(4)]
    triplet_node_reps = [node_rep(z) for node_rep in node_reps]
    node_pair_inversions = [(1, 2), (1, 3), (2, 3), (3, 1)]
    triplets = functools.reduce(
        lambda x, y: x + y,
        [
            jnp.expand_dims(tri_node_rep, axis=perm)
            for tri_node_rep, perm in zip(
                triplet_node_reps, node_pair_inversions
            )
        ],
    )
    return jnp.max(triplets, axis=1) - jnp.min(triplets, axis=1)
```

Listing 6. The triplet representation that we refer to as QUADNODEMINMAX.

```python
def get_triplet_msgs_concatrep(z, edge_fts, graph_fts, nb_triplet_fts, out_size):
    def rep_fn(x, size):
        proj = hk.nets.MLP([size])
        ff = hk.nets.MLP([size * 4, size])
        return jnp.concatenate([
            proj(x),
            ff(x),
        ], axis=-1)

    triplet_node_reps = [rep_fn(z, nb_triplet_fts) for _ in range(3)]
    triplet_edge_reps = [rep_fn(edge_fts, nb_triplet_fts) for _ in range(3)]
```

```
12    triplet_graph_rep = rep_fn(graph_fts, nb_triplet_fts)
13    node_pair_permutations = [(2, 3), (1, 3), (1, 2)]
14    triplets = functools.reduce(
15        lambda x, y: x + y,
16        [
17            jnp.expand_dims(tri_node_rep, axis=perm)
18            for tri_node_rep, perm in zip(
19                triplet_node_reps, node_pair_permutations
20            )
21        ],
22    )
23    triplets += functools.reduce(
24        lambda x, y: x + y,
25        [
26            jnp.expand_dims(tri_edge_rep, axis=i)
27            for tri_edge_rep, i in zip(triplet_edge_reps, range(3, 0, -1))
28        ],
29    )
30    triplets += jnp.expand_dims(triplet_graph_rep, axis=(1, 2, 3))
31    output_layer = hk.Linear(out_size)
32    return output_layer(jnp.max(triplets, axis=1))
```

Listing 7. The triplet representation that we refer to as CONCATREP.

```
1 def get_triplet_msgs_tanhexplandtriplets(z, edge_fts, graph_fts, nb_triplet_fts,
      out_size):
2   node_reps = [hk.Linear(nb_triplet_fts) for _ in range(3)]
3   edge_reps = [hk.Linear(nb_triplet_fts) for _ in range(3)]
4   graph_rep = hk.nets.MLP([nb_triplet_fts])
5   triplet_node_reps = [node_rep(z) for node_rep in node_reps]
6   triplet_edge_reps = [edge_rep(edge_fts) for edge_rep in edge_reps]
7   node_pair_permutations = [(2, 3), (1, 3), (1, 2)]
8   triplets = functools.reduce(
9       lambda x, y: x + y,
10      [
11          jnp.expand_dims(tri_node_rep, axis=perm)
12          for tri_node_rep, perm in zip(
13              triplet_node_reps, node_pair_permutations
14          )
15      ],
16  )
17  triplets += functools.reduce(
18      lambda x, y: x + y,
19      [
20          jnp.expand_dims(tri_edge_rep, axis=i)
21          for tri_edge_rep, i in zip(triplet_edge_reps, range(3, 0, -1))
22      ],
23  )
24  triplets += jnp.expand_dims(graph_rep(graph_fts), axis=(1, 2, 3))
25  triplets += jnp.expand_dims(graph_rep(graph_fts), axis=(2, 3, 1))
26  triplets += jnp.expand_dims(graph_rep(graph_fts), axis=(3, 1, 2))
27  output_layer = hk.Linear(out_size)
28  return output_layer(jnp.tanh(jnp.max(triplets, axis=1)))
```

Listing 8. The triplet representation that we refer to as TANHEXPANDTRIPLETS.

```
1 def get_triplet_msgs_div2mean(z, edge_fts, graph_fts, nb_triplet_fts, out_size):
2   node_reps = [hk.Linear(nb_triplet_fts) for _ in range(3)]
3   edge_reps = [hk.Linear(nb_triplet_fts) for _ in range(3)]
4   triplet_node_reps = [node_rep(z / 2) for node_rep in node_reps]
5   triplet_edge_reps = [edge_rep(edge_fts) for edge_rep in edge_reps]
```

```
 6    node_pair_permutations = [(2, 3), (1, 3), (1, 2)]
 7    triplets = functools.reduce(
 8        lambda x, y: x + y,
 9        [
10            jnp.expand_dims(tri_node_rep, axis=perm )
11            for tri_node_rep, perm in zip(
12                triplet_node_reps, node_pair_permutations
13            )
14        ],
15    )
16    triplets += functools.reduce(
17        lambda x, y: x + y,
18        [
19            jnp.expand_dims(tri_edge_rep, axis=perm)
20            for tri_edge_rep, perm in zip(triplet_edge_reps, range(3, 0, -1))
21        ],
22    )
23    output_layer = hk.Linear(out_size)
24    return output_layer(jnp.mean(triplets, axis=1))
```

Listing 9. The triplet representation that we refer to as DIV2MEAN.

```
 1 def get_triplet_msgs_maxmean(z, edge_fts, graph_fts, nb_triplet_fts, out_size):
 2    node_reps = [hk.Linear(nb_triplet_fts) for _ in range(3)]
 3    edge_reps = [hk.Linear(nb_triplet_fts) for _ in range(3)]
 4    graph_rep = hk.nets.MLP([nb_triplet_fts])
 5    triplet_node_reps = [node_rep(z) for node_rep in node_reps]
 6    triplet_edge_reps = [edge_rep(edge_fts) for edge_rep in edge_reps]
 7    node_pair_permutations = [(2, 3), (1, 3), (1, 2)]
 8    triplets = functools.reduce(
 9        lambda x, y: x + y,
10        [
11            jnp.expand_dims(tri_node_rep, axis=perm)
12            for tri_node_rep, perm in zip(
13                triplet_node_reps, node_pair_permutations
14            )
15        ],
16    )
17    triplets += functools.reduce(
18        lambda x, y: x + y,
19        [
20            jnp.expand_dims(tri_edge_rep, axis=i)
21            for tri_edge_rep, i in zip(triplet_edge_reps, range(3, 0, -1))
22        ],
23    )
24    triplets = jnp.maximum(triplets, -100.0)
25    output_layer = hk.Linear(out_size)
26    return output_layer(jnp.mean(triplets, axis=1))
```

Listing 10. The triplet representation that we refer to as MAXMEAN.

A.4. CLRS Seed Models

Below we provide the source code for the nine seed models used in the CLRS model search.

```python
def get_triplet_msgs_v1(z, edge_fts, graph_fts, nb_triplet_fts, out_size):
    node_reps = [hk.Linear(nb_triplet_fts) for _ in range(3)]
    edge_reps = [hk.Linear(nb_triplet_fts) for _ in range(3)]
    graph_rep = hk.Linear(nb_triplet_fts)
    triplet_node_reps = [node_rep(z) for node_rep in node_reps]
    triplet_edge_reps = [edge_rep(edge_fts) for edge_rep in edge_reps]
    triplet_graph_rep = graph_rep(graph_fts)
    node_pair_permutations = [(2, 3), (1, 3), (1, 2)]
    triplets = functools.reduce(
        lambda x, y: x + y,
        [
            jnp.expand_dims(tri_node_rep, axis=perm)
            for tri_node_rep, perm in zip(
                triplet_node_reps, node_pair_permutations
            )
        ],
    )
    triplets += functools.reduce(
        lambda x, y: x + y,
        [
            jnp.expand_dims(tri_edge_rep, axis=i)
            for tri_edge_rep, i in zip(triplet_edge_reps, range(3, 0, -1))
        ],
    )
    triplets += jnp.expand_dims(triplet_graph_rep, axis=(1, 2, 3))
    output_layer = hk.Linear(out_size)
    return output_layer(jnp.max(triplets, axis=1))
```

Listing 11. The triplet representation belonging to the first seed model - the standard triplet representation from Ibarz et al. (2022).

```python
def get_triplet_msgs_v2(z, edge_fts, graph_fts, nb_triplet_fts, out_size):
    node_reps = [hk.Linear(nb_triplet_fts) for _ in range(3)]
    edge_reps = [hk.Linear(nb_triplet_fts) for _ in range(3)]
    graph_rep = hk.Linear(nb_triplet_fts)
    triplet_node_reps = [node_rep(z) for node_rep in node_reps]
    triplet_edge_reps = [edge_rep(edge_fts) for edge_rep in edge_reps]
    triplet_graph_rep = graph_rep(graph_fts)
    node_pair_permutations = [(2, 3), (1, 3), (1, 2)]
    triplets = functools.reduce(
        lambda x, y: x + y,
        [
            jnp.expand_dims(tri_node_rep, axis=perm)
            for tri_node_rep, perm in zip(
                triplet_node_reps, node_pair_permutations
            )
        ],
    )
    triplets += functools.reduce(
        lambda x, y: x + y,
        [
            jnp.expand_dims(tri_edge_rep, axis=i)
            for tri_edge_rep, i in zip(triplet_edge_reps, range(3, 0, -1))
        ],
    )
    triplets += jnp.expand_dims(triplet_graph_rep, axis=(1, 2, 3))
    output_layer = hk.nets.MLP([out_size, out_size])
    return output_layer(jnp.max(triplets, axis=1))
```

Listing 12. The triplet representation belonging to the second seed model, with the output layer replaced by a fully-connected multi-layer perceptron.

```
1  def get_triplet_msgs_v3(z, edge_fts, graph_fts, nb_triplet_fts, out_size):
2    node_reps = [hk.Linear(nb_triplet_fts) for _ in range(3)]
3    edge_reps = [hk.Linear(nb_triplet_fts) for _ in range(3)]
4    graph_rep = hk.Linear(nb_triplet_fts)
5    triplet_node_reps = [node_rep(z) for node_rep in node_reps]
6    triplet_edge_reps = [edge_rep(edge_fts) for edge_rep in edge_reps]
7    triplet_graph_rep = graph_rep(graph_fts)
8    node_pair_permutations = [(2, 3), (1, 3), (1, 2)]
9    triplets = functools.reduce(
10       lambda x, y: x + y,
11       [
12           jnp.expand_dims(tri_node_rep, axis=perm)
13           for tri_node_rep, perm in zip(
14               triplet_node_reps, node_pair_permutations
15           )
16       ],
17   )
18   triplets += functools.reduce(
19       lambda x, y: x + y,
20       [
21           jnp.expand_dims(tri_edge_rep, axis=i)
22           for tri_edge_rep, i in zip(triplet_edge_reps, range(3, 0, -1))
23       ],
24   )
25   triplets += jnp.expand_dims(triplet_graph_rep, axis=(1, 2, 3))
26   output_layer = hk.Linear(out_size)
27   return output_layer(jnp.sum(triplets, axis=1))
```

Listing 13. The triplet representation belonging to the third seed model, which uses sum instead of max aggregation.

```
1  def get_triplet_msgs_v4(z, edge_fts, graph_fts, nb_triplet_fts, out_size):
2    node_reps = [hk.nets.MLP([nb_triplet_fts, nb_triplet_fts]) for _ in range(3)]
3    edge_reps = [hk.Linear(nb_triplet_fts) for _ in range(3)]
4    graph_rep = hk.Linear(nb_triplet_fts)
5    triplet_node_reps = [node_rep(z) for node_rep in node_reps]
6    triplet_edge_reps = [edge_rep(edge_fts) for edge_rep in edge_reps]
7    triplet_graph_rep = graph_rep(graph_fts)
8    node_pair_permutations = [(2, 3), (1, 3), (1, 2)]
9    triplets = functools.reduce(
10       lambda x, y: x + y,
11       [
12           jnp.expand_dims(tri_node_rep, axis=perm)
13           for tri_node_rep, perm in zip(
14               triplet_node_reps, node_pair_permutations
15           )
16       ],
17   )
18   triplets += functools.reduce(
19       lambda x, y: x + y,
20       [
21           jnp.expand_dims(tri_edge_rep, axis=i)
22           for tri_edge_rep, i in zip(triplet_edge_reps, range(3, 0, -1))
23       ],
24   )
25   triplets += jnp.expand_dims(triplet_graph_rep, axis=(1, 2, 3))
26   output_layer = hk.Linear(out_size)
```

```
27    return output_layer(jnp.max(triplets, axis=1))
```

Listing 14. The triplet representation of the 4th seed model, which uses fully-connected multi-layer perceptron node representations.

```
1  def get_triplet_msgs_v5(z, edge_fts, graph_fts, nb_triplet_fts, out_size):
2    node_reps = [hk.Linear(nb_triplet_fts) for _ in range(3)]
3    edge_reps = [hk.nets.MLP([nb_triplet_fts, nb_triplet_fts]) for _ in range(3)]
4    graph_rep = hk.Linear(nb_triplet_fts)
5    triplet_node_reps = [node_rep(z) for node_rep in node_reps]
6    triplet_edge_reps = [edge_rep(edge_fts) for edge_rep in edge_reps]
7    triplet_graph_rep = graph_rep(graph_fts)
8    node_pair_permutations = [(2, 3), (1, 3), (1, 2)]
9    triplets = functools.reduce(
10       lambda x, y: x + y,
11       [
12           jnp.expand_dims(tri_node_rep, axis=perm)
13           for tri_node_rep, perm in zip(
14               triplet_node_reps, node_pair_permutations
15           )
16       ],
17   )
18   triplets += functools.reduce(
19       lambda x, y: x + y,
20       [
21           jnp.expand_dims(tri_edge_rep, axis=i)
22           for tri_edge_rep, i in zip(triplet_edge_reps, range(3, 0, -1))
23       ],
24   )
25   triplets += jnp.expand_dims(triplet_graph_rep, axis=(1, 2, 3))
26   output_layer = hk.Linear(out_size)
27   return output_layer(jnp.max(triplets, axis=1))
```

Listing 15. The triplet representation of the 5th seed model, which uses fully-connected multi-layer perceptron edge representations.

```
1  def get_triplet_msgs_v6(z, edge_fts, graph_fts, nb_triplet_fts, out_size):
2    node_reps = [hk.Linear(nb_triplet_fts) for _ in range(3)]
3    edge_reps = [hk.Linear(nb_triplet_fts) for _ in range(3)]
4    graph_rep = hk.nets.MLP([nb_triplet_fts, nb_triplet_fts])
5    triplet_node_reps = [node_rep(z) for node_rep in node_reps]
6    triplet_edge_reps = [edge_rep(edge_fts) for edge_rep in edge_reps]
7    triplet_graph_rep = graph_rep(graph_fts)
8    node_pair_permutations = [(2, 3), (1, 3), (1, 2)]
9    triplets = functools.reduce(
10       lambda x, y: x + y,
11       [
12           jnp.expand_dims(tri_node_rep, axis=perm)
13           for tri_node_rep, perm in zip(
14               triplet_node_reps, node_pair_permutations
15           )
16       ],
17   )
18   triplets += functools.reduce(
19       lambda x, y: x + y,
20       [
21           jnp.expand_dims(tri_edge_rep, axis=i)
22           for tri_edge_rep, i in zip(triplet_edge_reps, range(3, 0, -1))
23       ],
24   )
25   triplets += jnp.expand_dims(triplet_graph_rep, axis=(1, 2, 3))
```

```
26    output_layer = hk.Linear(out_size)
27    return output_layer(jnp.max(triplets, axis=1))
```

Listing 16. The triplet representation of the 6th seed model, which uses fully-connected multi-layer perceptron graph representations.

```
1  def get_triplet_msgs_v7(z, edge_fts, graph_fts, nb_triplet_fts, out_size):
2    node_reps = [hk.nets.MLP([nb_triplet_fts]) for _ in range(3)]
3    edge_reps = [hk.Linear(nb_triplet_fts) for _ in range(3)]
4    triplet_node_reps = [node_rep(z) for node_rep in node_reps]
5    triplet_edge_reps = [edge_rep(edge_fts) for edge_rep in edge_reps]
6    node_pair_permutations = [(2, 3), (1, 3), (1, 2)]
7    triplets = functools.reduce(
8        lambda x, y: x + y,
9        [
10            jnp.expand_dims(tri_node_rep, axis=perm)
11            for tri_node_rep, perm in zip(
12                triplet_node_reps, node_pair_permutations
13            )
14        ],
15    )
16    triplets += functools.reduce(
17        lambda x, y: x + y,
18        [
19            jnp.expand_dims(tri_edge_rep, axis=i)
20            for tri_edge_rep, i in zip(triplet_edge_reps, range(3, 0, -1))
21        ],
22    )
23    output_layer = hk.Linear(out_size)
24    return output_layer(jnp.max(triplets, axis=1))
```

Listing 17. The triplet representation of the 7th seed model, which uses fully-connected multi-layer perceptron node representations and does not have a graph representation.

```
1  def get_triplet_msgs_v8(z, edge_fts, graph_fts, nb_triplet_fts, out_size):
2    output_layer = hk.nets.MLP([out_size])
3    return jnp.tile(
4        jnp.expand_dims(output_layer(z), axis=(1)), [1, z.shape[1], 1, 1]
5    )
```

Listing 18. The triplet representation of the 8th seed model, which simply applies a linear layer and tiles the output to maintain dimensional consistency.

```
1  def get_triplet_msgs_v9(z, edge_fts, graph_fts, nb_triplet_fts, out_size):
2    def rep_fn(x, size):
3      proj = hk.nets.MLP([size])
4      ff = hk.nets.MLP([size * 8, size])
5      return proj(x) * ff(x)
6
7    triplet_node_reps = [rep_fn(z, nb_triplet_fts) for _ in range(3)]
8    triplet_edge_reps = [rep_fn(edge_fts, nb_triplet_fts) for _ in range(3)]
9    triplet_graph_rep = rep_fn(graph_fts, nb_triplet_fts)
10   node_pair_permutations = [(2, 3), (1, 3), (1, 2)]
11   triplets = functools.reduce(
12       lambda x, y: x + y,
13       [
14           jnp.expand_dims(tri_node_rep, axis=perm)
15           for tri_node_rep, perm in zip(
```

```
16                  triplet_node_reps, node_pair_permutations
17              )
18          ],
19      )
20      triplets += functools.reduce(
21          lambda x, y: x + y,
22          [
23              jnp.expand_dims(tri_edge_rep, axis=i)
24              for tri_edge_rep, i in zip(triplet_edge_reps, range(3, 0, -1))
25          ],
26      )
27      triplets += jnp.expand_dims(triplet_graph_rep, axis=(1, 2, 3))
28      return rep_fn(jnp.max(triplets, axis=1), out_size)
```

Listing 19. The triplet representation of the 9th seed model, which uses a bilinear representation for the node, edge, and graph representations.

A.5. OOD Evaluation of Newly Discovered Models on CLRS

Table 3. A full list comparing 5 of the newly discovered GNNs against the baseline Triplet-GMPNN model from Ibarz et al. (2022) on all 30 of the CLRS (Veličković et al., 2022) tasks. For the baseline, we include the OOD accuracy of both our implementation of the Triplet-GMPNN as well as the number listed in the original paper.

Algorithm	Best Performing Model	Model Size (number of parameters) ↓		OOD Accuracy ↑		
		Best Performing Model	Baseline model	Best performing newly discovered model	Baseline model (our implementation)	Baseline model (from Ibarz et al. (2022))
Activity Selector	Baseline	262204	262204	95.05 ± 0.53%	93.96± 0.29%	95.18± 0.45%
Articulation Points	QUADNODEMINMAX	497969	531913	93.46 ± 1.77%	91.40± 1.74%	88.32± 2.01%
Bellman Ford	CONCATREP	568660	524604	97.50 ± 0.31%	97.08± 0.24%	97.39± 0.19%
BFS	MAXMEAN	522931	523963	99.99 ± 0.01%	99.80± 0.04%	99.73± 0.04%
Binary Search	Baseline	262204	262204	77.98 ± 2.49%	79.57± 1.73%	77.58± 2.35%
Bridges	CONCATREP	576612	532556	97.57 ± 1.08%	97.31± 1.11%	93.99± 2.07%
Bubble Sort	CONCATREP	568533	524477	88.87 ± 2.77%	83.20± 4.27%	67.68± 5.50%
DAG Shortest Paths	Baseline	793287	793287	98.01 ± 0.22%	97.48± 0.37%	98.19± 0.30%
DFS	DIV2MEAN	660158	661190	68.14 ± 1.38%	46.78± 3.85%	47.79± 4.19%
Dijkstra	DIV2MEAN	524854	525886	97.30 ± 0.28%	95.94± 0.66%	96.05± 0.60%
Find Maximum Subarray Kadane	Baseline	261290	264514	75.35 ± 0.92%	74.09± 0.83%	76.36± 0.43%
Floyd Warshall	CONCATREP	669145	625089	61.43 ± 0.79%	48.95± 0.49%	48.52± 1.04%
Graham Scan	MAXMEAN	397377	398409	93.76 ± 0.85%	92.72± 2.38%	93.62± 0.91%
Heapsort	CONCATREP	703710	659654	69.90 ± 4.17%	19.45± 5.35%	31.04± 5.82%
Insertion Sort	DIV2MEAN	523445	524477	89.47 ± 2.57%	86.89± 1.89%	78.14± 4.64%
Jarvis March	Baseline	308954	264898	90.36 ± 0.65%	88.91± 0.91%	91.01± 1.30%
Knuth-Morris-Pratt	Baseline	396989	398021	16.29 ± 4.36%	8.88± 1.76%	19.51± 4.57%
LCS Length	Baseline	270419	270419	85.75 ± 0.80%	86.05± 0.65%	80.51± 1.84%
Matrix Chain Order	Baseline	624448	624448	90.77 ± 0.75%	91.15± 0.85%	91.68± 0.59%
Minimum	DIV2MEAN	260275	261307	98.40 ± 0.16%	98.26± 0.26%	97.78± 0.55%
Mst Kruskal	CONCATREP	443747	399691	91.47 ± 0.48%	90.60± 0.32%	89.80± 0.77%
Mst Prim	CONCATREP	569942	525886	88.74 ± 1.67%	85.18± 2.24%	86.39± 1.33%
Naive String Matcher	QUADNODEMINMAX	259364	262588	79.77 ± 2.88%	73.39± 6.33%	78.67± 4.99%
Optimal Bst	DIV2MEAN	624955	625987	78.66 ± 0.46%	78.08± 0.96%	73.77± 1.48%
Quickselect	QUADNODEMINMAX	377130	395714	0.79 ± 0.41%	0.13± 0.08%	0.47± 0.25%
Quicksort	DIV2MEAN	524727	525759	85.23 ± 4.26%	84.71± 2.66%	64.64± 5.12%
Segments Intersect	DIV2MEAN	262327	263359	98.15 ± 0.00%	97.40± 0.00%	97.64± 0.09%
Strongly Connected Components	Baseline	707299	663243	41.86 ± 3.39%	43.71± 5.94%	43.43± 3.15%
Task Scheduling	TANHEXPANDTRIPLETS	262333	262333	88.23 ± 0.44%	88.10± 0.31%	87.25± 0.35%
Topological Sort	TANHEXPANDTRIPLETS	660164	660164	88.12 ± 4.71%	76.88± 5.05%	87.27± 2.67%